

**In-situ Growth of Porous TiO₂ with Controllable Oxygen Vacancies at Atomic
Scale for Highly Efficient Photocatalytic Water Splitting**

*Fan Yang^{a, b}, Ruizhuang Yang^a, Lin Yan^a, Xiaolin Liu^{a, b}, Xuan Luo^{*a} and Lin Zhang^{a, b}*

^a Science and Technology on Plasma Physics Laboratory, Research Center of Laser Fusion, China Academy of Engineering Physics, Mianyang, Sichuan 621900, P.R. China

^b Department of Physics, University of Science and Technology of China, Hefei, Anhui 230026, P.R. China

Table S1 Lattice information and grain size of as-prepared TiO₂ from XRD Rietveld refinement

samples	a=b (Å)	c (Å)	Grain size (nm)
Ti-5-O-0.1	3.803 (1)	9.611 (8)	18.1
Ti-1-O-0.1	3.805 (7)	9.614 (5)	17.9
Ti-0.1-O-0.1	3.810 (0)	9.613 (5)	18.0
Ti-0.1-O-1	3.826 (8)	9.648 (2)	18.4
Ti-0.1-O-5	3.836 (2)	9.677 (3)	18.0

The XRD Rietveld refinement implied the lattice constant of porous TiO₂ decreased from 3.836 and 9.677 Å to 3.803 and 9.611 Å with the ratio of Ti and O precursors' pulse time increase. This change trend of TiO₂ lattice originated from the lack of O atom and introduction of oxygen vacancies. The lattice relaxation due to the lack of O atom would strengthen the Ti-O bond, thus lead to the shrinkage of TiO₂ lattice. Meanwhile, the grain size of all as-prepared TiO₂ materials had negligible difference, indicating the same phase change under deposition and calcining process.

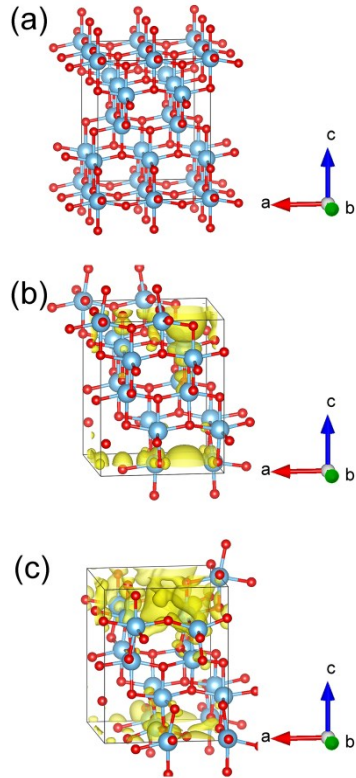


Figure S1 The partial charge density at conduction band edge of (a) perfect anatase TiO₂ crystal, (b) TiO₂ crystal with an oxygen vacancy and (c) TiO₂ crystal with two oxygen vacancies. The red and cyan spheres represent O and Ti atoms, respectively.

Figure S1 revealed that the electrons at conduction band edge accelerated at vicinity of oxygen vacancies. The introduced oxygen vacancies would promote the electrons-holes separation and transfer.

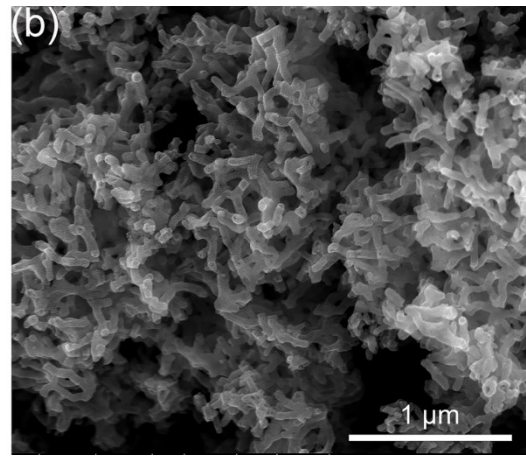
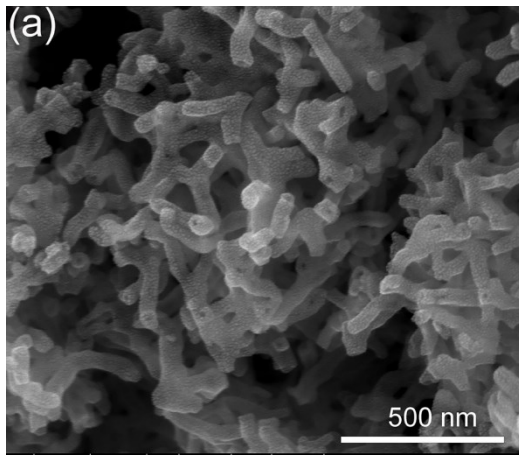


Figure S2 the SEM images of Ti-5-O-0.1

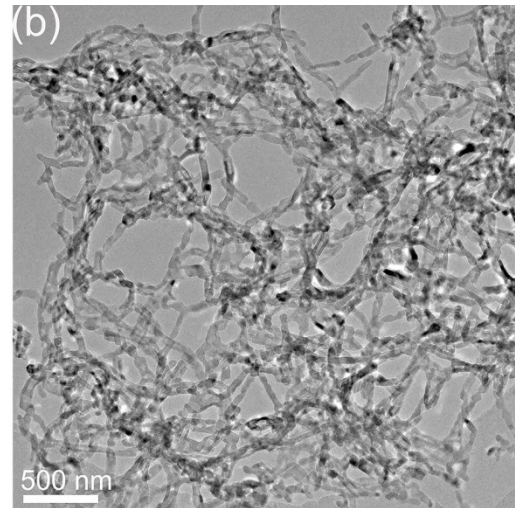
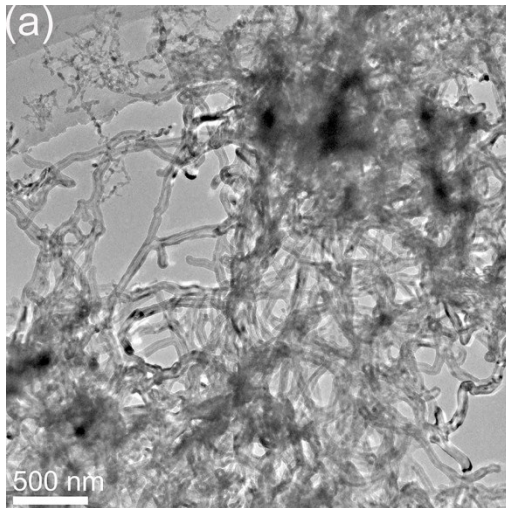


Figure S3 the low- magnification TEM images of Ti-5- O-0.1 (a) and Ti-0.1-O-5 (b)

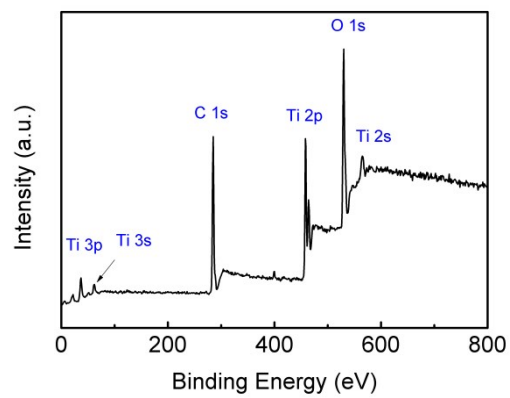


Figure S4 the XPS survey of Ti-5-O-0.1 sample

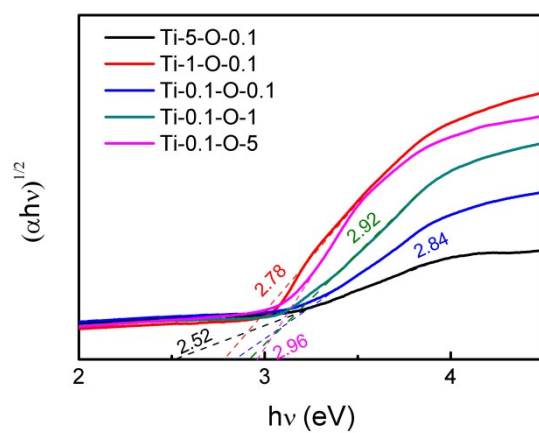


Figure S5 The tauc plots of five as-prepared porous TiO_2 from the UV-Vis diffuse reflectance spectra.

The band gap E_g estimated from the optical measurement showed a blue shift trend with the increase of oxygen vacancies. Based on theoretical calculation, the introduction of oxygen vacancy would bring in new defect level and shift the defect level to valence band, resulting in the narrowed TiO_2 band gap.

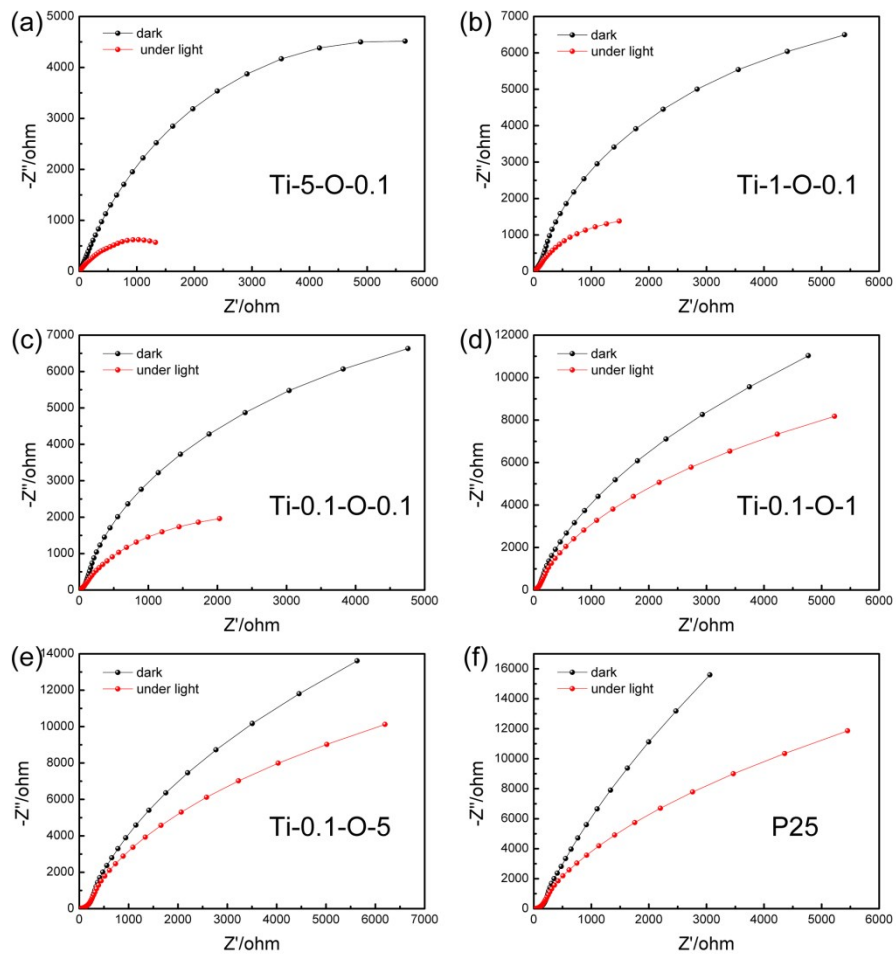


Figure S6 EIS curves under light on/off of five porous TiO_2 materials and commercial P25

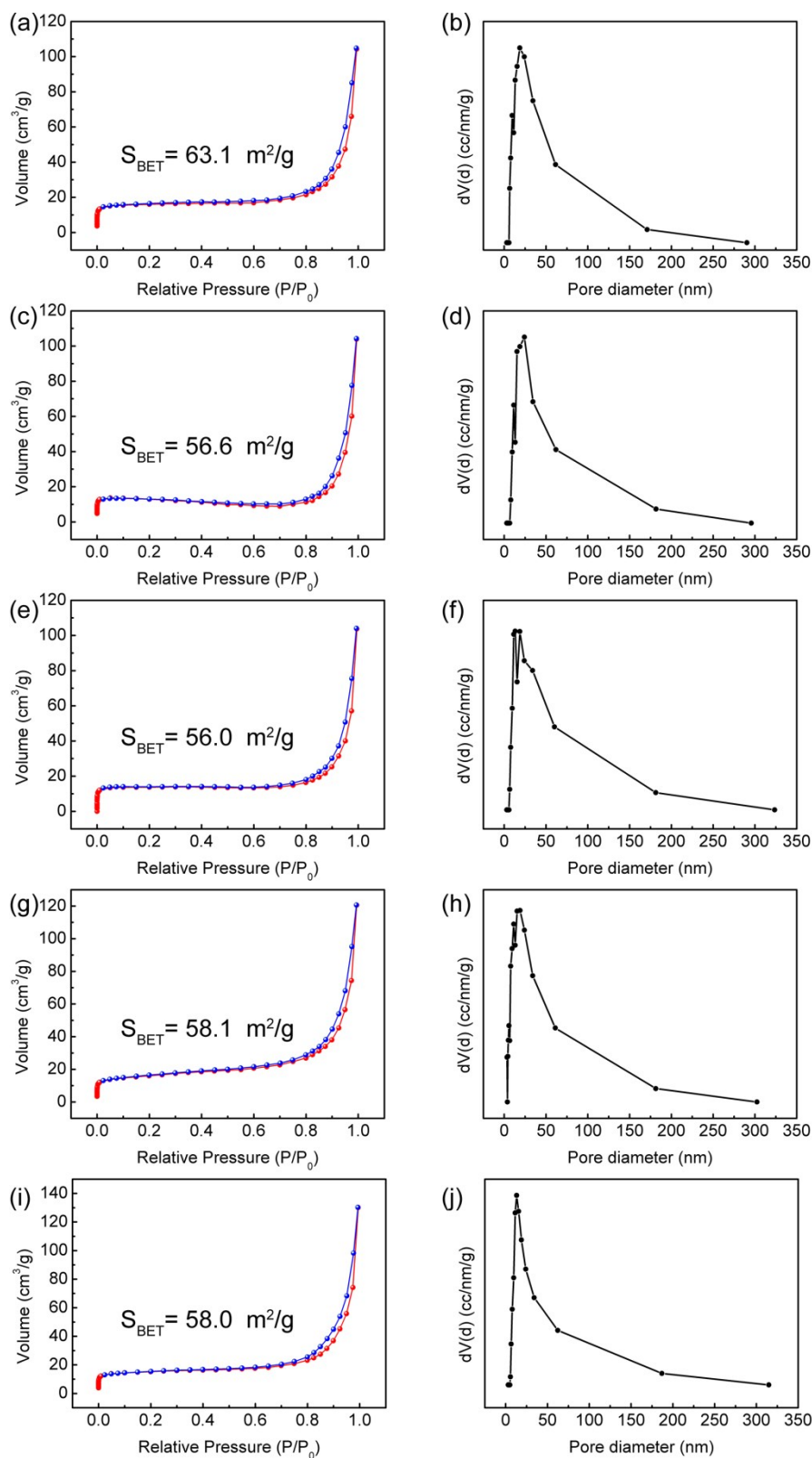


Figure S7 the N₂ absorption/desorption isotherm curves and relevant BJH pore size distribution of Ti-5-O-0.1 (a-b), Ti-1-O-0.1(c-d), Ti-0.1-O-0.1(e-f), Ti-0.1-O-1(g-h) and Ti-0.1-O-5(i-j), respectively.

The pore size distribution curves showed that all samples possessed almost similar pore structure with the main pore at 18-22 nm.

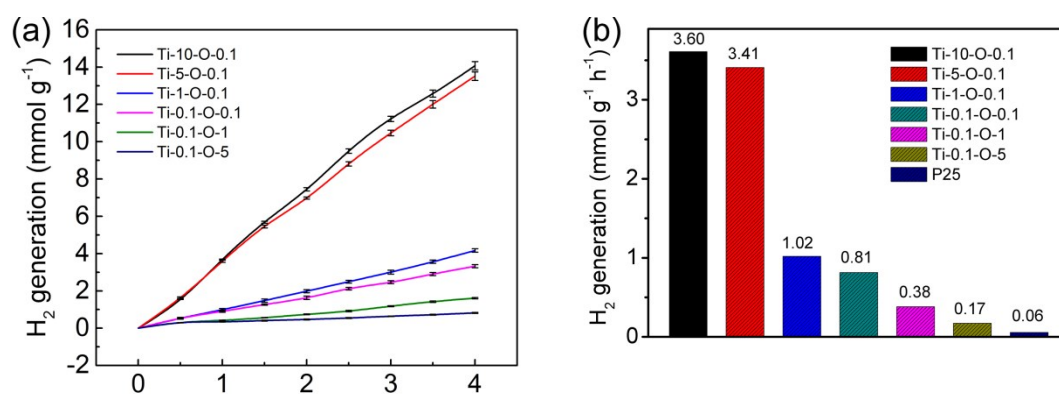


Figure S8 The photocatalytic H₂ generation rate diagram of six porous TiO₂ and commercial P25

We prepared six different porous TiO₂ materials with varying precursors' pulse time. From photocatalytic H₂ generation measurement, there was minor difference between Ti-10-O-0.1 and Ti-5-O-0.1 compared with other four TiO₂ materials. This indicated that further increase of Ti precursor's pulse time had limited influence on concentration of oxygen vacancies and photocatalytic property. Based on that, we chose the Ti-5-O-0.1 sample as the V_o abundant TiO₂ in whole experiments.